

Measurement of the branching fraction for the decay $\Upsilon(4S) \rightarrow \Upsilon(1S)\pi^+\pi^-$

A. Sokolov,¹⁴ M. Shapkin,¹⁴ H. Aihara,⁴⁴ K. Arinstein,^{1,32} T. Aushev,^{15,20} A. M. Bakich,³⁹ E. Barberio,²² A. Bay,²⁰ K. Belous,¹⁴ V. Bhardwaj,³⁴ A. Bondar,^{1,32} M. Bračko,^{16,21} T. E. Browder,⁹ M.-C. Chang,⁵ P. Chang,²⁷ A. Chen,²⁵ K.-F. Chen,²⁷ B. G. Cheon,⁸ C.-C. Chiang,²⁷ R. Chistov,¹⁵ I.-S. Cho,⁴⁹ Y. Choi,³⁸ M. Dash,⁴⁸ A. Drutskoy,³ W. Dungel,¹³ S. Eidelman,^{1,32} D. Epifanov,^{1,32} N. Gabyshev,^{1,32} P. Goldenzweig,³ H. Ha,¹⁸ J. Haba,¹⁰ B.-Y. Han,¹⁸ H. Hayashii,²⁴ M. Hazumi,¹⁰ Y. Horii,⁴³ Y. Hoshi,⁴² W.-S. Hou,²⁷ Y. B. Hsiung,²⁷ H. J. Hyun,¹⁹ T. Iijima,²³ K. Inami,²³ A. Ishikawa,³⁵ H. Ishino,^{45,*} Y. Iwasaki,¹⁰ N. J. Joshi,⁴⁰ D. H. Kah,¹⁹ H. Kaji,²³ J. H. Kang,⁴⁹ H. Kawai,² T. Kawasaki,³⁰ H. Kichimi,¹⁰ H. J. Kim,¹⁹ H. O. Kim,¹⁹ S. K. Kim,³⁷ Y. I. Kim,¹⁹ Y. J. Kim,⁷ K. Kinoshita,³ B. R. Ko,¹⁸ S. Korpar,^{16,21} P. Križan,^{16,50} P. Krokovny,¹⁰ A. Kuzmin,^{1,32} Y.-J. Kwon,⁴⁹ S.-H. Kyeong,⁴⁹ J. S. Lange,⁶ M. J. Lee,³⁷ S. E. Lee,³⁷ T. Lesiak,^{4,28} J. Li,⁹ A. Limosani,²² S.-W. Lin,²⁷ Y. Liu,²³ D. Liventsev,¹⁵ R. Louvot,²⁰ F. Mandl,¹³ A. Matyja,²⁸ S. McOnie,³⁹ H. Miyata,³⁰ Y. Miyazaki,²³ R. Mizuk,¹⁵ T. Mori,²³ Y. Nagasaka,¹¹ E. Nakano,³³ M. Nakao,¹⁰ S. Nishida,¹⁰ O. Nitoh,⁴⁷ S. Noguchi,²⁴ S. Ogawa,⁴¹ T. Ohshima,²³ S. Okuno,¹⁷ H. Ozaki,¹⁰ P. Pakhlov,¹⁵ G. Pakhlova,¹⁵ C. W. Park,³⁸ H. Park,¹⁹ H. K. Park,¹⁹ K. S. Park,³⁸ R. Pestotnik,¹⁶ L. E. Piilonen,⁴⁸ A. Poluektov,^{1,32} H. Sahoo,⁹ Y. Sakai,¹⁰ O. Schneider,²⁰ C. Schwanda,¹³ A. Sekiya,²⁴ K. Senyo,²³ M. E. Sevior,²² C. P. Shen,⁹ J.-G. Shiu,²⁷ B. Shwartz,^{1,32} J. B. Singh,³⁴ S. Stanič,³¹ M. Starič,¹⁶ T. Sumiyoshi,⁴⁶ M. Tanaka,¹⁰ G. N. Taylor,²² Y. Teramoto,³³ T. Tsuboyama,¹⁰ S. Uehara,¹⁰ T. Uglov,¹⁵ Y. Unno,⁸ S. Uno,¹⁰ Y. Usov,^{1,32} G. Varner,⁹ K. E. Varvell,³⁹ K. Vervink,²⁰ A. Vinokurova,^{1,32} C. H. Wang,²⁶ M.-Z. Wang,²⁷ P. Wang,¹² X. L. Wang,¹² Y. Watanabe,¹⁷ R. Wedd,²² E. Won,¹⁸ B. D. Yabsley,³⁹ Y. Yamashita,²⁹ C. Z. Yuan,¹² Z. P. Zhang,³⁶ V. Zhilich,^{1,32} V. Zhulanov,^{1,32} T. Zivko,¹⁶ A. Zupanc,¹⁶ and O. Zyukova^{1,32}

(Belle Collaboration)

¹*Budker Institute of Nuclear Physics, Novosibirsk*²*Chiba University, Chiba*³*University of Cincinnati, Cincinnati, Ohio 45221*⁴*T. Kościuszko Cracow University of Technology, Krakow*⁵*Department of Physics, Fu Jen Catholic University, Taipei*⁶*Justus-Liebig-Universität Gießen, Gießen*⁷*The Graduate University for Advanced Studies, Hayama*⁸*Hanyang University, Seoul*⁹*University of Hawaii, Honolulu, Hawaii 96822*¹⁰*High Energy Accelerator Research Organization (KEK), Tsukuba*¹¹*Hiroshima Institute of Technology, Hiroshima*¹²*Institute of High Energy Physics, Chinese Academy of Sciences, Beijing*¹³*Institute of High Energy Physics, Vienna*¹⁴*Institute of High Energy Physics, Protvino*¹⁵*Institute for Theoretical and Experimental Physics, Moscow*¹⁶*J. Stefan Institute, Ljubljana*¹⁷*Kanagawa University, Yokohama*¹⁸*Korea University, Seoul*¹⁹*Kyungpook National University, Taegu*²⁰*École Polytechnique Fédérale de Lausanne (EPFL), Lausanne*²¹*University of Maribor, Maribor*²²*University of Melbourne, School of Physics, Victoria 3010*²³*Nagoya University, Nagoya*²⁴*Nara Women's University, Nara*²⁵*National Central University, Chung-li*²⁶*National United University, Miao Li*²⁷*Department of Physics, National Taiwan University, Taipei*²⁸*H. Niewodniczanski Institute of Nuclear Physics, Krakow*²⁹*Nippon Dental University, Niigata*³⁰*Niigata University, Niigata*³¹*University of Nova Gorica, Nova Gorica*³²*Novosibirsk State University, Novosibirsk*

*Now at Okayama University, Okayama.

³³*Osaka City University, Osaka*³⁴*Panjab University, Chandigarh*³⁵*Saga University, Saga*³⁶*University of Science and Technology of China, Hefei*³⁷*Seoul National University, Seoul*³⁸*Sungkyunkwan University, Suwon*³⁹*University of Sydney, Sydney, New South Wales*⁴⁰*Tata Institute of Fundamental Research, Mumbai*⁴¹*Toho University, Funabashi*⁴²*Tohoku Gakuin University, Tagajo*⁴³*Tohoku University, Sendai*⁴⁴*Department of Physics, University of Tokyo, Tokyo*⁴⁵*Tokyo Institute of Technology, Tokyo*⁴⁶*Tokyo Metropolitan University, Tokyo*⁴⁷*Tokyo University of Agriculture and Technology, Tokyo*⁴⁸*IPNAS, Virginia Polytechnic Institute and State University, Blacksburg, Virginia 24061*⁴⁹*Yonsei University, Seoul*⁵⁰*Faculty of Mathematics and Physics, University of Ljubljana, Ljubljana*

(Received 13 January 2009; published 20 March 2009)

We study transitions between Y states with the emission of charged pions using 604.6 fb^{-1} of data collected with the Belle detector at the KEKB asymmetric-energy e^+e^- collider. The measured product branching fraction is $\mathcal{B}(Y(4S) \rightarrow Y(1S)\pi^+\pi^-) \times \mathcal{B}(Y(1S) \rightarrow \mu^+\mu^-) = (2.11 \pm 0.30(\text{stat}) \pm 0.14(\text{sys})) \times 10^{-6}$ and the partial decay width is $\Gamma(Y(4S) \rightarrow Y(1S)\pi^+\pi^-) = (1.75 \pm 0.25(\text{stat}) \pm 0.24(\text{sys})) \text{ keV}$.

DOI: 10.1103/PhysRevD.79.051103

PACS numbers: 13.25.Gv, 14.60.Ef, 14.40.Aq

The bottomonium state $Y(4S)$ has a mass above the threshold for $B\bar{B}$ pair production and decays mainly into B -meson pairs [$\mathcal{B}(Y(4S) \rightarrow B\bar{B}) > 96\%$ [1]]. Recently, the decay modes $Y(4S) \rightarrow Y(mS)\pi\pi$ with $m = 1, 2$ as well as $Y(4S) \rightarrow \eta Y(1S)$ [2] have also been observed. These decays as well as the anomalously large width of the $Y(5S) \rightarrow Y(mS)\pi\pi$ ($m = 1, 2, 3$) transitions discovered by Belle [3] give additional information about various QCD models that are used to describe hadronic transitions of heavy quarkonia [4]. Preliminary evidence for the decay $Y(4S) \rightarrow Y(1S)\pi^+\pi^-$ was presented by the Belle Collaboration in Ref. [5]. The BABAR Collaboration reported measurements of the $Y(4S)$ transition to the $Y(1S)$ or $Y(2S)$ with the emission of a $\pi^+\pi^-$ pair [2,6]. The first Belle measurements of $Y(4S) \rightarrow Y(1S)\pi^+\pi^-$ were published in Ref. [7]. The product branching fraction $\mathcal{B}(Y(4S) \rightarrow Y(1S)\pi^+\pi^-) \times \mathcal{B}(Y(1S) \rightarrow \mu^+\mu^-)$ from Belle differs by 2.4 standard deviations from the corresponding value from BABAR [2]. In this paper we present a new study of the decay mode $Y(4S) \rightarrow Y(1S)\pi^+\pi^-$ from the Belle experiment using a larger data sample and relaxed signal selection criteria.

We use 604.6 fb^{-1} of data collected on the $Y(4S)$ resonance with the Belle detector [8] at the KEKB asymmetric-energy e^+e^- collider [9]. We study $Y(4S) \rightarrow Y(1S)\pi^+\pi^-$ decays with a subsequent $Y(1S) \rightarrow \mu^+\mu^-$ transition. Charged particles are reconstructed and identified in the Belle detector, which consists of a silicon vertex detector (SVD), central drift chamber (CDC), aerogel threshold Cherenkov counters (ACC), time-of-flight (TOF) scintilla-

tion counters, an electromagnetic calorimeter (ECL), and a K_L -muon detector (KLM).

Charged tracks must originate from within a region of radius 1 cm and axial length ± 5 cm centered in the e^+e^- interaction point and not be associated with a well-reconstructed K_S^0 meson, Λ baryon, or converted photon; each charged track should have a momentum transverse to the beam axis (p_T) of greater than $0.1 \text{ GeV}/c$. Charged particles are assigned a likelihood \mathcal{L}_i [10] ($i = \mu, \pi, K$) based on the matching of hits in the KLM to the track extrapolated from the CDC, and identified as muons if the likelihood ratio $P_\mu = \mathcal{L}_\mu / (\mathcal{L}_\mu + \mathcal{L}_\pi + \mathcal{L}_K)$ exceeds 0.8, corresponding to a muon detection efficiency of approximately 91.5% over the polar angle range $20^\circ \leq \theta \leq 155^\circ$ and the momentum range $0.7 \text{ GeV}/c \leq p \leq 3.0 \text{ GeV}/c$ in the laboratory frame. Electron identification uses a similar likelihood ratio P_e [11] based on CDC, ACC, and ECL information. Charged particles that are not identified as muons and have a likelihood ratio $P_e < 0.1$ are treated as pions. Calorimeter clusters not associated with reconstructed charged tracks and with energies greater than 50 MeV are classified as photon candidates.

Candidates for $Y(4S) \rightarrow Y(1S)\pi^+\pi^-$ decays with the subsequent leptonic decay $Y(1S) \rightarrow \mu^+\mu^-$ are selected from the standard hadronic-event sample for the first 492 fb^{-1} data set (sample I), while an additional τ -enriched sample is also used for the remaining 113 fb^{-1} data set (sample II). The relevant selection criteria for the standard hadronic-event sample are the following: three or more charged tracks; a visible energy E_{vis} of at

least $0.2\sqrt{s}$, where \sqrt{s} is the center-of-mass (c.m.) energy; a calorimeter energy deposit in the range $0.1 \leq E_{\text{sum}}/\sqrt{s} \leq 0.8$; and a maximum of $0.5\sqrt{s}$ for the magnitude of P_z , the sum of the z components of the momenta of each charged track and neutral cluster, where the z axis is defined to be the direction opposite to the positron beam. The variables E_{vis} , E_{sum} , and P_z are evaluated in the c.m. system.

Unfortunately, the hadronic-event sample criterion $E_{\text{sum}}/\sqrt{s} \geq 0.1$ rejects a considerable fraction of our signal events. However, some of these lost events are recovered in the τ -enriched sample because it has a loose constraint on the E_{sum} variable ($E_{\text{sum}} \leq 10$ GeV). Only the newest τ -enriched data are used because the earlier subset included a requirement on the sum of the magnitudes of the charged track momenta in the c.m. frame (below 10 GeV/c) that rejected most of our signal. Other selection criteria for the τ -enriched sample, while not critical for this study, are enumerated below. The number of charged tracks in an event should be greater than 1 and less than 9 with zero net charge. The maximum p_T among the tracks is required to be greater than 0.5 GeV/c. Beam-related background is rejected by requiring that the position of the reconstructed event vertex be less than 1 cm from the interaction point (IP) in the transverse direction and less than 3 cm from the IP along the beam direction. To suppress background from Bhabha and $\mu^+\mu^-$ events, the maximum opening angle between charge tracks is required to be less than 175° in the CM frame.

To select $Y(4S) \rightarrow Y(1S)\pi^+\pi^-$ decays, an event is required to contain exactly four charged tracks with a $\mu^+\mu^-$ pair having an invariant mass $M_{\mu\mu}$ above 9.0 GeV/c² and a $\pi^+\pi^-$ pair whose opening angle $\theta_{\pi\pi}$ in the laboratory frame satisfies $\cos\theta_{\pi\pi} < 0.95$. The latter criterion suppresses the radiative return process [12] $e^+e^- \rightarrow Y(1S)\gamma$ as well as $e^+e^- \rightarrow \mu^+\mu^-\gamma$, wherein the photon converts to an e^+e^- pair that is misidentified as a pion pair. Poorly reconstructed events are discarded by requiring a visible energy in the laboratory frame of 10.5 GeV $< E_{\text{vis}}^{\text{lab}} < 12.5$ GeV.

To identify parent resonances that decay into the $Y(1S)\pi^+\pi^-$ final state, the distribution of $M_{\mu\mu}$ vs the mass difference $\Delta M = M_{\mu\mu\pi\pi} - M_{\mu\mu}$ is examined (see Fig. 1) for the selected data sample. The cluster of events in the parallelogram centered at $(\Delta M, M_{\mu\mu}) = (1.12, 9.46)$ GeV/c² is from the transition $Y(4S) \rightarrow Y(1S)\pi^+\pi^-$. The other clusters are due to the decays $Y(2S) \rightarrow Y(1S)\pi^+\pi^-$ and $Y(3S) \rightarrow Y(1S)\pi^+\pi^-$, where the $Y(2S)$ and $Y(3S)$ are produced predominantly by radiative return, i.e. $e^+e^- \rightarrow Y(mS)\gamma$.

The rightmost cluster in Fig. 1 contains events from the process $Y(4S) \rightarrow Y(1S)\pi^+\pi^-$. The dominant background processes, $e^+e^- \rightarrow \mu^+\mu^-\gamma$ ($\gamma \rightarrow e^+e^-$), $e^+e^- \rightarrow \mu^+\mu^-\mu^+\mu^-$, and $e^+e^- \rightarrow \mu^+\mu^-\pi^+\pi^-$, accumulate at the kinematic boundary indicated by the diagonal line in Fig. 1. To capture the $Y(4S) \rightarrow Y(1S)\pi^+\pi^-$ signal as well

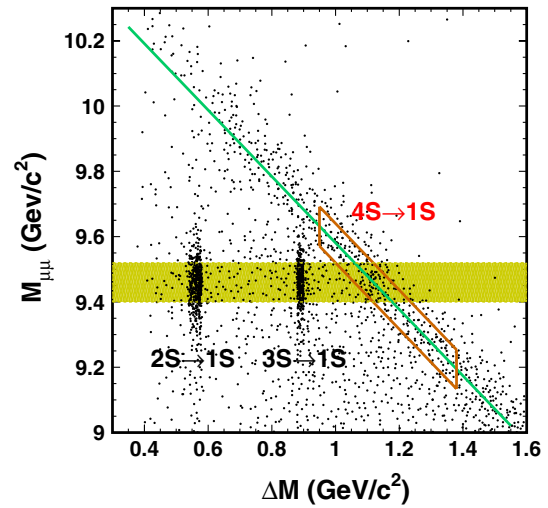


FIG. 1 (color online). The $M_{\mu\mu}$ vs ΔM distribution for the candidate events. The ± 60 MeV high horizontal shaded band is centered on the nominal $Y(1S)$ mass. The clusters on the lower left correspond to $Y(2S) \rightarrow Y(1S)\pi^+\pi^-$ and $Y(3S) \rightarrow Y(1S)\pi^+\pi^-$ transitions. The diagonal line indicates the kinematic boundary $M_{\mu\mu\pi\pi} = \sqrt{s}$. The parallelogram straddling this line defines the fitting region for $Y(4S) \rightarrow Y(1S)\pi^+\pi^-$ candidates.

as estimate this background more reliably, we fit the distribution of ΔM for events within the parallelogram of Fig. 1, whose boundaries correspond to $|M_{\mu\mu\pi\pi} - \sqrt{s}| < 60$ MeV/c² and 950 MeV/c² $< \Delta M < 1380$ MeV/c². The fit, shown in Fig. 2, includes a Gaussian for the signal and a quadratic function for the background. The fitted Gaussian is centered at (1118.7 ± 1.2) MeV/c², which is

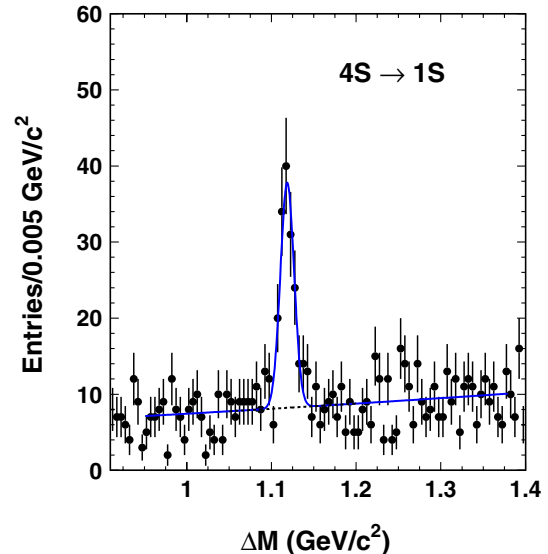


FIG. 2 (color online). The fit to the ΔM distribution for events within the parallelogram of Fig. 1 using a Gaussian for the signal and a second-order polynomial for the background (dotted line). The solid curve shows the sum of the Gaussian and the polynomial function.

in good agreement with the nominal $m_{Y(4S)} - m_{Y(1S)}$ mass difference, and has a width of (8.1 ± 1.0) MeV/ c^2 , which is consistent with the detector's estimated ΔM resolution. The signal yield in the interval 1105 MeV/ $c^2 < \Delta M < 1135$ MeV/ c^2 , determined as the difference of the number of events and the fitted background in this interval, is $N_{\text{ev}} = 113.7 \pm 16.3$, with a statistical significance of 11.2σ , corresponding to $-2 \ln(\mathcal{L}_0/\mathcal{L}_{\text{max}}) = 135.0$ with three fit parameters (mass, width, and yield). Here, \mathcal{L}_0 and \mathcal{L}_{max} are the likelihood values returned by the fit with the signal yield fixed at zero and its best fit value, respectively.

Additional information can be obtained from the study of the $\pi^+\pi^-$ system. Background-subtracted and efficiency-corrected distribution of $\pi^+\pi^-$ invariant mass ($M_{\pi\pi}$) is shown in Fig. 3 for events within the signal subregion (1105 MeV/ $c^2 < \Delta M < 1135$ MeV/ c^2) of the parallelogram in Fig. 1. (The background is estimated from the sideband subregion 950 MeV/ $c^2 < \Delta M < 1075$ MeV/ c^2 and 1175 MeV/ $c^2 < \Delta M < 1350$ MeV/ c^2). The EVTGEN event generator [13], with a matrix element that accounts for particle spins [14], is used to produce $Y(4S) \rightarrow Y(1S)\pi^+\pi^- \rightarrow \mu^+\mu^-\pi^+\pi^-$ events that are then passed through the detector simulation [15] and reconstruction programs.

The $M_{\pi\pi}$ distribution in Fig. 3 can be described using the shape predicted by the models of Ref. [14], in which suppression of small $\pi^+\pi^-$ invariant masses follows from partial conservation of axial current. The goodness of fit, for 10 degrees of freedom, is $\chi^2/\text{NDF} = 0.35$.

The branching fraction for the $Y(4S) \rightarrow Y(1S)\pi^+\pi^-$ decay is determined from $\mathcal{B}(Y(4S) \rightarrow Y(1S)\pi^+\pi^-) = N_{\text{ev}}/(N_{Y(4S)} \cdot \varepsilon \cdot \mathcal{B}(Y(1S) \rightarrow \mu^+\mu^-))$, where N_{ev} is the

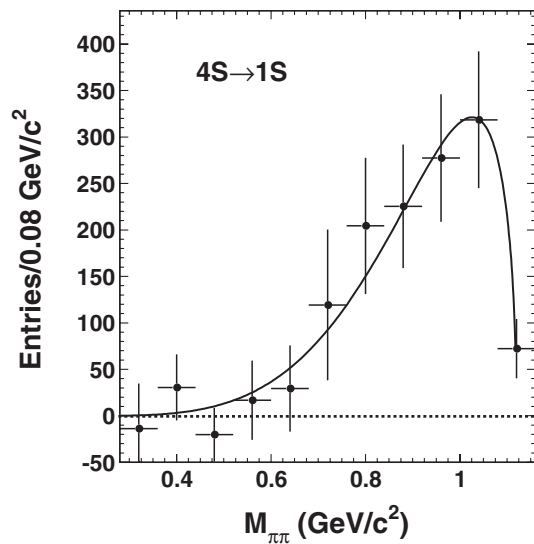


FIG. 3. Background-subtracted and efficiency-corrected distribution of $\pi^+\pi^-$ invariant mass ($M_{\pi\pi}$) for events within the signal subregion of the parallelogram in Fig. 1. The solid curve shows the $M_{\pi\pi}$ distribution predicted by the models of Ref. [14].

extracted signal yield, $N_{Y(4S)}$ is the estimated number of $Y(4S)$ events produced, ε is the signal detection efficiency (calculated separately for samples I and II), and $\mathcal{B}(Y(1S) \rightarrow \mu^+\mu^-) = (2.48 \pm 0.05)\%$ is the PDG-tabulated branching fraction for the daughter decay. The efficiencies are calculated from Monte Carlo simulations. For the hadronic-event simulation in sample I, we apply a correction to E_{sum}/\sqrt{s} , one of the variables used to select hadronic events, so that this distribution agrees with that of the data. This correction is also applied to sample II, where it changes the efficiency by a few percent. The results are given in Table I.

The systematic error in the reconstruction efficiency due to the last correction is 8% for sample I and essentially zero for sample II. The systematic uncertainty in the reconstruction efficiency due to lack of knowledge of the $Y(4S) \rightarrow Y(1S)\pi^+\pi^- \rightarrow \mu^+\mu^-\pi^+\pi^-$ decay matrix element is estimated by comparing the parametrization of the $M_{\pi\pi}$ distribution in the models of Ref. [14] and in a phase space model. We estimate this systematic uncertainty as half of the variation in the efficiency, and it is equal to 2.0% (3.1%); here and below, the first (second) value gives the systematic uncertainty for sample I (sample II). The signal yield is extracted by an unbinned extended maximum likelihood fit to the ΔM distribution for events in the parallelogram (Fig. 1) using a Gaussian for the signal and a second-order polynomial for the background. The signal yield in the signal interval 1105 MeV/ $c^2 < \Delta M < 1135$ MeV/ c^2 is determined as the difference of the number of events and the fitted background in this interval. The signal yield from the fitted Gaussian area has a larger statistical error. The systematic uncertainties from the discrepancies between these two evaluations of the signal yield are 2.2% and 1.2% for samples I and II, respectively. Other systematic uncertainties come from the choice of the fit range (0.3%, 2.5%), the choice of the signal range (2%, 0.6%), the choice of the signal box width (2.4%, 1.9%), the change of the order of the polynomial function from two to one (0.5%, 1.2%), the tracking efficiency (4%, 4%), the muon identification efficiency (1.1%, 1.1%), the pion identification efficiency (0.2%, 0.2%), the statistical uncertainty in the efficiency (1.0%, 0.6%), the uncertainty in the $Y(1S) \rightarrow \mu^+\mu^-$ decay branching fraction (2.0%, 2.0%), and the total number of $Y(4S)$ events (1.3%, 1.1%). The total systematic uncertainty for each data sample is obtained by adding these contributions in quadrature; the results are 10.3% and 6.6% for samples I and II,

TABLE I. Total number of $Y(4S)$ ($N_{Y(4S)}$), signal yield (N_{ev}), reconstruction efficiency (ε), and branching fraction (\mathcal{B}) for the $Y(4S) \rightarrow Y(1S)\pi^+\pi^-$ decay.

Data sample	$N_{Y(4S)}, 10^6$	N_{ev}	$\varepsilon, \%$	$\mathcal{B}, 10^{-4}$
I	534.6 ± 7.0	52.2 ± 10.7	4.5	0.86 ± 0.18
II	122.1 ± 1.4	61.3 ± 12.1	25.1	0.84 ± 0.17

respectively. The systematic uncertainties from the tracking efficiency, $Y(4S)$ counting, $\mathcal{B}(Y(1S) \rightarrow \mu^+ \mu^-)$, and muon and pion identification efficiencies are treated as fully correlated systematic errors for samples I and II. Other uncertainties are treated as uncorrelated errors. First the weighted average of the uncorrelated uncertainties $\langle \sigma_{\text{sys}}^{\text{uncor}} \rangle$ is evaluated. The total systematic uncertainty is obtained by adding $\langle \sigma_{\text{sys}}^{\text{uncor}} \rangle$ and the remaining correlated uncertainties in quadrature.

The measured weighted product branching fraction is

$$\begin{aligned} \mathcal{B}(Y(4S) \rightarrow Y(1S)\pi^+\pi^-) \times \mathcal{B}(Y(1S) \rightarrow \mu^+\mu^-) \\ = (2.11 \pm 0.30(\text{stat}) \pm 0.14(\text{sys})) \times 10^{-6}. \end{aligned}$$

The branching fraction is

$$\begin{aligned} \mathcal{B}(Y(4S) \rightarrow Y(1S)\pi^+\pi^-) \\ = (0.85 \pm 0.12(\text{stat}) \pm 0.06(\text{sys})) \times 10^{-4}. \end{aligned}$$

We also extract the partial decay width for the $Y(4S) \rightarrow Y(1S)\pi^+\pi^-$ transition using the world-average value of the total width [1], and obtain

$$\begin{aligned} \Gamma(Y(4S) \rightarrow Y(1S)\pi^+\pi^-) \\ = (1.75 \pm 0.25(\text{stat}) \pm 0.24(\text{sys})) \text{ keV}. \end{aligned}$$

The measured values of $\mathcal{B}(Y(4S) \rightarrow Y(1S)\pi^+\pi^-)$ and $\Gamma(Y(4S) \rightarrow Y(1S)\pi^+\pi^-)$ supersede our previous results [7] with improved accuracy. The new Belle results are compatible with those of *BABAR* [2].

To summarize, a study of transitions between Y states with the emission of charged pions has been performed by Belle. The peak at $\Delta M = (1118.7 \pm 1.2) \text{ MeV}/c^2$ is interpreted as a signal for the decay $Y(4S) \rightarrow Y(1S)\pi^+\pi^-$ with a subsequent $Y(1S) \rightarrow \mu^+\mu^-$ transition. The branch-

ing fraction $\mathcal{B}(Y(4S) \rightarrow Y(1S)\pi^+\pi^-)$ and the partial decay width $\Gamma(Y(4S) \rightarrow Y(1S)\pi^+\pi^-)$ are measured. We have not studied the $Y(4S) \rightarrow Y(2S)\pi^+\pi^-$ decay because criteria applied to the raw experimental data make our sensitivity to this decay limited.

We thank the KEKB group for the excellent operation of the accelerator, the KEK cryogenics group for the efficient operation of the solenoid, and the KEK computer group and the National Institute of Informatics for valuable computing and SINET3 network support. We acknowledge support from the Ministry of Education, Culture, Sports, Science, and Technology (MEXT) of Japan, the Japan Society for the Promotion of Science (JSPS), and the Tau-Lepton Physics Research Center of Nagoya University; the Australian Research Council and the Australian Department of Industry, Innovation, Science and Research; the National Natural Science Foundation of China under Contract No. 10575109, No. 10775142, No. 10875115, and No. 10825524; the Department of Science and Technology of India; the BK21 program of the Ministry of Education of Korea, the CHEP SRC program and Basic Research program (Grant No. R01-2008-000-10477-0) of the Korea Science and Engineering Foundation; the Polish Ministry of Science and Higher Education; the Ministry of Education and Science of the Russian Federation and the Russian Federal Agency for Atomic Energy; the Slovenian Research Agency; the Swiss National Science Foundation; the National Science Council and the Ministry of Education of Taiwan; and the U.S. Department of Energy. This work is supported by a Grant-in-Aid from MEXT for Science Research in a Priority Area (“New Development of Flavor Physics”), and from JSPS for Creative Scientific Research (“Evolution of Tau-lepton Physics”).

-
- [1] C. Amsler *et al.* (Particle Data Group), *Phys. Lett. B* **667**, 1 (2008).
- [2] B. Aubert *et al.* (*BABAR* Collaboration), *Phys. Rev. D* **78**, 112002 (2008).
- [3] K.-F. Chen *et al.* (Belle Collaboration), *Phys. Rev. Lett.* **100**, 112001 (2008).
- [4] E. Eichten *et al.*, *Rev. Mod. Phys.* **80**, 1161 (2008); Y. P. Kuang, *Front. Phys. China* **1**, 19 (2006); Yu. A. Simonov, *JETP Lett.* **87**, 147 (2008); C. Meng and K. T. Chao, *Phys. Rev. D* **77**, 074003 (2008).
- [5] K. Abe *et al.* (Belle Collaboration), arXiv:hep-ex/0512034.
- [6] B. Aubert *et al.* (*BABAR* Collaboration), *Phys. Rev. Lett.* **96**, 232001 (2006).
- [7] A. Sokolov *et al.* (Belle Collaboration), *Phys. Rev. D* **75**, 071103 (2007).
- [8] A. Abashian *et al.* (Belle Collaboration), *Nucl. Instrum. Methods Phys. Res., Sect. A* **479**, 117 (2002).
- [9] S. Kurokawa and E. Kikutani, *Nucl. Instrum. Methods Phys. Res., Sect. A* **499**, 1 (2003), and other papers included in this volume.
- [10] A. Abashian *et al.* (Belle Collaboration), *Nucl. Instrum. Methods Phys. Res., Sect. A* **491**, 69 (2002).
- [11] K. Hanagaki *et al.*, *Nucl. Instrum. Methods Phys. Res., Sect. A* **485**, 490 (2002).
- [12] M. Benayoun *et al.*, *Mod. Phys. Lett. A* **14**, 2605 (1999).
- [13] D. J. Lange, *Nucl. Instrum. Methods Phys. Res., Sect. A* **462**, 152 (2001).
- [14] L. S. Brown and R. N. Cahn, *Phys. Rev. Lett.* **35**, 1 (1975); M. B. Voloshin, *JETP Lett.* **21**, 347 (1975); T.-M. Yan, *Phys. Rev. D* **22**, 1652 (1980).
- [15] R. Brun, R. Hagelberg, M. Hansroul, and J. C. Lassalle, Report No. CERN-DD-78-2-REV 1, 1978.